BIOMOLECULES & THERAPEUTICS

Original Article
Biomol Ther 31(3), 330-339 (2023)

Liver Kinase B1 Mediates Its Anti-Tumor Function by Binding to the N-Terminus of Malic Enzyme 3

Seung Bae Rho[1,*], Hyun Jung Byun[2], Boh-Ram Kim[2] and Chang Hoon Lee[2,*]

[1]Division of Cancer Biology, Research Institute, National Cancer Center, Goyang 10408,
[2]College of Pharmacy, Dongguk University, Goyang 10326, Republic of Korea

Abstract

Liver kinase B1 (LKB1) is a crucial tumor suppressor involved in various cellular processes, including embryonic development, tumor initiation and progression, cell adhesion, apoptosis, and metabolism. However, the precise mechanisms underlying its functions remain elusive. In this study, we demonstrate that LKB1 interacts directly with malic enzyme 3 (ME3) through the N-terminus of the enzyme and identified the binding regions necessary for this interaction. The binding activity was confirmed to promote the expression of ME3 in an LKB1-dependent manner and was also shown to induce apoptosis activity. Furthermore, LKB1 and ME3 overexpression upregulated the expression of tumour suppressor proteins (p53 and p21) and downregulated the expression of antiapoptotic proteins (nuclear factor kappa-light-chain-enhancer of activated B cells (NF-κB) and B-cell lymphoma 2 (Bcl-2)). Additionally, LKB1 and ME3 enhanced the transcription of p21 and p53 and inhibited the transcription of NF-κB. Moreover, LKB1 and ME3 suppressed the phosphorylation of various components of the phosphatidylinositol-4,5-bisphosphate 3-kinase/protein kinase B signaling pathway. Overall, these results suggest that LKB1 promotes pro-apoptotic activities by inducing ME3 expression.

Key Words: LKB1, Pro-apoptosis, Protein-protein interaction, Cell cycle, Ovarian tumorigenesis, ME3

INTRODUCTION

Liver kinase B1 (LKB1), also known as the serine/threonine kinase 11 (STK11) gene, is a widely expressed tumor suppressor gene that is commonly associated with Peutz-Jeghers syndrome (PJS) (Avilés-Salas *et al*., 2023; Omori *et al*., 2023). It plays a crucial role in regulating multiple cellular processes, including tumor initiation and progression (Gao *et al*., 2010; Hardie, 2013), invasion, and adhesion (Zagórska *et al*., 2010; Konen *et al*., 2016), energy metabolism (Bhatt *et al*., 2023), cell cycle (Gurumurthy *et al*., 2010), cell migration, and embryonic development (Men *et al*., 2015). LKB1 functions as a master regulator by directly phosphorylating the AMP-activated protein kinase (AMPK) family of proteins, thereby modulating their activity (Shackelford and Shaw, 2009; Zhang *et al*., 2013). Mutations in the LKB1 gene have been identified in several types of cancer tissues, including non-small cell lung, ovarian, cervical, endometrial, breast, pancreatic, and thyroid carcinomas, and have also been implicated in various mouse models of cancer (Shackelford and Shaw, 2009; Zhao and Xu, 2014; Wei *et al*., 2016; Katipally *et al*., 2023).

AMP-activated protein kinase (AMPK) is a critical enzyme involved in the regulation of various cellular processes including cell growth, homeostasis, and metabolism, as well as autophagy control (Rho *et al*., 2021). The enzyme is a highly conserved heterotrimeric complex consisting of α catalytic subunits (α1 and α2) and β (β1 and β2) and γ (γ1, γ2, and γ3) regulatory subunits (Mihaylova and Shaw, 2011). AMPK has been implicated in various physiological and pathological conditions, including cancer, diabetes, Alzheimer's disease, inflammation, aging, and metabolic syndrome. Activation of AMPK has been shown to be beneficial for treating these diseases, and is promoted by the commonly prescribed oral anti-diabetic agent, metformin. AMPK activity is regulated by adenoside diphosphate (ADP)/adenosine triphosphate (ATP) and adenosine monophosphate (AMP)/ATP ratios, with binding of AMP and ADP to the γ subunit protecting AMPK against dephosphorylation and promoting its phosphorylation (Steinberg and Kemp, 2009; Hardie *et al*., 2012; Oakhill *et al*., 2012). AMPK is also regulated by phosphorylation of a threonine residue (Thr172) in the catalytic subunit, as well as by the ubiquitin proteasome system, protein translation, and

Open Access **https://doi.org/10.4062/biomolther.2023.041**

Received Mar 1, 2023 **Revised** Mar 18, 2023 **Accepted** Mar 24, 2023
Published Online May 1, 2023

***Corresponding Authors**
E-mail: sbrho@ncc.re.kr (Rho SB), uatheone@dongguk.edu (Lee CH)
Tel: +82-31-920-2383 (Rho SB), +82-31-961-5213 (Lee CH)
Fax: +82-31-920-2399 (Rho SB), +82-31-961-5206 (Lee CH)

autophagy (Huynh *et al*., 2016). These multiple pathways suggest the complexity and importance of AMPK in maintaining cellular homeostasis.

Malic enzymes (MEs) are a family of enzymes that are present in a wide range of species, from bacteria to humans, and are involved in various biological processes, such as metabolism, photosynthesis, and fatty acid biosynthesis (Dmitriev, 2001). In mammals, three isoforms of ME have been identified: ME1, ME2, and ME3 (Chang and Tong, 2003; Hasan *et al*., 2015; Wang *et al*., 2021). While ME1 is distributed in the cytosol, ME2 and ME3 are found in the mitochondria. These enzymes are homotetramers, and their amino acid sequences are highly conserved, with approximately 68% sequence identity (Hasan *et al*., 2015). The oxidative decarboxylation of L-malate to pyruvate while simultaneously reducing NAD(P)+ to NAD(P)H is catalyzed by MEs (Cheng *et al*., 2016), which are essential for the regulation of the cellular redox status (Costa Rosa *et al*., 1995) and for biosynthetic processes, including lipid and fatty acid synthesis (Infante and Huszagh, 1998; Dmitriev, 2001). The enzymatic activity of ME proteins is inhibited by ATP and is activated by fumarate (Yang *et al*., 2002). ME1 and ME2 are abundant in pancreatic islets and insulin cells, while the mRNA levels and enzymatic activity of ME3 are low in these cells (Hasan *et al*., 2015).

Several studies have reported on the roles of malic enzyme isoforms in tumorigenesis. For example, ME1 suppression has been shown to reduce metastasis of hepatocellular carcinoma by repressing the epithelial-mesenchymal transition in reactive oxygen species-induced signaling cascades (Wen *et al*., 2015). Similarly, ME2 depletion induces erythroid differentiation in human K562 erythroleukemia cells (Ren *et al*., 2010) and apoptotic cell death and differentiation in lung tumor cells, and also suppresses Akt phosphorylation and activity (Ren *et al*., 2014). ME2 has also been shown to be a potential target for inhibiting tumor growth and invasiveness in various tumor cell types, including lung and melanoma cancer cells (Cheng *et al*., 2016; Zhang *et al*., 2023). In contrast, little is known about the role of ME3 in ovarian tumorigenesis. Further investigation is necessary to elucidate the potential involvement of ME3 in ovarian cancer development and progression.

In this study, we aimed to investigate the functional importance and molecular mechanism of ME3 in LKB1-induced apoptotic cell death in an *in vitro* experimental model system to address the pivotal role of LKB1 in human ovarian tumors. Our observations provide insights into the cellular mechanisms through which ME3 contributes to LKB1-stimulated apoptosis in ovarian tumorigenesis.

MATERIALS AND METHODS

Culture conditions, chemicals, and antibodies

Human OVCAR-3 ovarian carcinoma cells and human embryonic kidney cells 293 (HEK293T) were obtained from the American Type Culture Collection (ATCC, Manassas, VA, USA), and were maintained in Dulbecco's Modified Eagle Medium (DMEM; Life Technologies, Gaithersburg, MD, USA) supplemented with 10% heat-inactivated fetal bovine serum (FBS) and penicillin/streptomycin. Wortmannin and LY294002 were purchased from Sigma (St. Louis, MO, USA). The primary antibodies used in this study were anti-LKB1, anti-ME3, anti-NF-κB, anti-Bcl-2, anti-p53, anti-PI3K, anti-phospho-PI3K, anti-Akt, anti-phospho-Akt (Ser473 and Thr308), anti-PDK-1, anti-phospho-PDK1 (Ser241), anti-mTOR, anti-phospho-mTOR (Ser2448), anti-TSC2, and anti-phospho-TSC2 (Ser1462), anti-p70S6K, anti-phospho-p70S6K (Thr421), anti-GSK-3β, anti-phospho-GSK-3β (Ser9), anti-4E-BP1, anti-phospho-4E-BP1 (Thr70) (Cell Signaling, Beverly, MA), anti-Flag, anti-cyclin D1, anti-CDK4, anti-p21 (Santa Cruz Biotechnology, Santa Cruz, CA, USA), and β-actin (Sigma).

Yeast two-hybrid (Y2H) assay

The cDNA encoding the full-length and truncation mutants (Met^{1}–Ala^{200}, Leu^{201}–Asp^{350}, and Glu^{351}–Gln^{433}) of LKB1 were subcloned in the pGilda/LexA yeast shuttle vector at the *Eco*RI and *Xho*I restriction enzyme sites. The full-length ME3 and three truncation mutants (Met^{1}–Tyr^{200}, Gly^{201}–Glu^{400}, and Glu^{401}–Val^{604}) were introduced into the pJG4-5 vector to generate B42 fusion proteins at the *Eco*RI and *Xho*I sites. The bait pGilda/LexA-LKB1 plasmid was transformed into the yeast strain EGY48 using a modified lithium acetate protocol (Rho *et al*., 2020). The ME3 cDNAs encoding pJG4-5 fusion proteins were transformed into yeast competent cells that already contained pGilda/LexA-LKB1, and the transformants were selected based on their tryptophan prototrophy (plasmid marker) on a synthetic medium (uracil, histidine, and tryptophan) containing 2% (w/v) glucose. The relative binding of the interaction was measured as previously described (Rho *et al*., 2020).

Co-immunoprecipitation and western blot

The co-immunoprecipitation (co-IP) assays were performed as previously described (Kang *et al*., 2022). Briefly, cells were trypsinized, centrifuged, and the pellets were washed with cold phosphate-buffered saline and resuspended in lysis buffer [50 mM Tris-HCl pH 7.2, 150 mM NaCl, 1% Triton X-100, and a protease inhibitor cocktail containing 1 μg/mL leupeptin, 1 μg/mL pepstatin, 2 μg/mL aprotinin, and 200 μg/mL phenylmethylsulfonyl fluoride (PMSF)]. The cell lysates were incubated with anti-Flag antibody and precipitated with protein A-agarose (GE Healthcare Life Sciences, Piscataway, NJ, USA). Approximately 20-25 g precipitated protein was separated by 10-12% sodium dodecyl sulfate polyacrylamide gel electrophoresis (SDS-PAGE) and transferred to Immobilon P membrane (Millipor Corporation, Billerica, MA, USA). After blocking, the membranes were incubated with specific primary antibodies. The membranes were rinsed three times with Tris-buffered saline with Tween buffer for 5 min, and incubated with horseradish peroxidase-conjugated secondary antibodies for 1 h at room temperature. The protein blots were exposed using an enhanced chemiluminescence detection system (GE Healthcare Life Sciences). Protein levels were measured using ImageQuant 5.0 software (Molecular Dynamics Inc., Sunnyvale, CA, USA) and normalized to levels of the loading control (β-actin). Values below the blots indicate relative ratios compared to the controls.

Apoptotic cell death assay

Cells were grown in chamber slides at a density of 4.5×10^{4} cells per well, transfected, incubated with fluorescein isothiocyanate (FITC)-labeled annexin V and propidium iodide for 15 min according to the manufacturer's instructions (BD PharMingen, Mississauga, ON, USA), and analyzed with a FACS Vantage (BD FACS Calibur Flow Cytometer, BD, Andover, MA, USA). Cell viability was estimated with the MTT

assay. Cells were maintained at a density of 4.5×10^3 cells per well in 96-well plates. Fresh medium including 10% FBS and 20 μL of 3-(4,5-dimethylthiazol-2-yl)-2.5-diphenyl-^{2}H-tetrazolium bromide (MTT) solution (5 μg/mL; Sigma) was added to each well 3 d following transfection, and each well was incubated for an additional 4 h at 37°C. Following centrifugation at 500×*g* for 10 min, the supernatant was removed from the wells and the formazan was dissolved with DMSO. The amount of MTT formazan generated was measured as an absorbance of 540 nm using a microplate reader (SpectraMax, Molecular Devices, Sunnyvale, CA, USA).

Caspase-3 activity

Caspase-3 activity was measured as previously described (Rho *et al*., 2021). Briefly, 3.1×10^5 cells were grown in 60 cm^2 culture dishes. After apoptosis was induced, the cells were harvested by centrifugation, and the pellets were re-suspended in lysis buffer and incubated with caspase-3-specific fluorometric substrates at 37°C for 1 h. A SpectraMax 340 microplate reader (Molecular Devices, Sunnyvale, CA, USA) was used to analyze caspase-3 activity.

Luciferase activity assay

Luciferase activity *in vitro* was assayed as previously described (Rho *et al*., 2022). Briefly, cells were grown to 85% confluency and co-transfected with promoter luciferase plasmids containing the *Renilla* luciferase reporter (Promega, Madison, WI, USA) for 24 h. Following lysis with radioimmunoprecipitation buffer, the lysates were cleared by centrifugation at 14,000 rpm for 15 min, and the cell extracts were incubated with the luciferase substrate reagent at room temperature for 30 min according to the manufacturer's instructions. Then, a 5 μL aliquot of each sample was quantified using a MicroLumat Plus LB96V luminometer (Berthold Technologies, Bad Wildbad, Germany). The ratio was normalized for *Renilla* luciferase activity to correct for variation in transfection efficiency.

PI3K activity

In vitro kinase assays were performed as described previously (Rho *et al*., 2011). Briefly, the cells were seeded at a density of 1.4×10^6 cells. Following overnight incubation, cells were treated with various concentrations of doxazosin for 6 h, and lysed in 1% NP-40 lysis buffer containing 20 mM Tris-HCl pH 7.5, 100 mM NaCl, 1 mM EDTA, 1 mM $MgCl_2$, 1% NP-40, 1 mM PMSF, and 0.1 mM sodium orthovanadate. After removal of the insoluble materials by centrifugation, the supernatants were incubated for 1 h at 4°C with anti-p85 antibody, followed by incubation with protein A-agarose beads for an additional 1 h at 4°C. The immunoprecipitates were incubated with a kinase reaction mixture containing 200 μg/mL phosphatidylinositol 3-phosphate and 2 μCi of [^{32}P] ATP per assay at 37°C for 15 min. The reaction products were visualized by autoradiography and the radioactive lipids were quantified by liquid scintillation counting.

Statistical analysis

Data values were expressed as the mean ± standard deviation (SD) and were estimated by Student's *t*-tests and analyses of variance according to the number of groups compared. Significant differences ($p<0.05$) are depicted with asterisks in each figure. The analyses were performed with SPSS 20 software (Statistical Product and Service Solutions, Chicago, IL, USA).

RESULTS

The tumor suppressor LKB1 directly interacts with ME3

The study utilized a yeast two-hybrid (Y2H) protein-protein interaction (PPI) system and co-immunoprecipitation (co-IP) to investigate the molecular mechanism underlying the tumor suppressive effect of LKB1 in ovarian tumorigenesis.

ME3 was identified as a putative binding partner of LKB1 in the human ovary cDNA library through Y2H screening (accession number: BC022472.2; Fig. 1A).

The relative binding of LKB1 to ME3 was confirmed by the activity of β-galactosidase in yeast cells co-expressing LKB1 and ME3. As shown in Fig. 1B, β-galactosidase was fully active with LKB1 and ME3 (82.08 ± 1.22), but failed in the absence of LKB1 (1.84 ± 0.51).

Co-IP experiments were performed to further confirm the direct interaction between LKB1 and ME3 in OVCAR-3 cells. LKB1 (pcDNA3.1/LKB1) and ME3 (pcDNA3.1/Flag-ME3) or ME3 (pcDNA3.1/Flag-ME3) and the expression vector (pcDNA3.1) only were co-transfected into OVCAR-3 cells, and immunoprecipitation of the lysates was performed with anti-Flag antibody. The precipitated proteins were immunoblotted with the anti-LKB1 or anti-ME3 primary antibodies, and the results indicated that Flag-ME3 co-immunoprecipitated with LKB1 (lane 2 in upper panel) (Fig. 1C).

The *in vivo* interaction between endogenous LKB1 and ME3 was also confirmed by co-IP in HEK293T cells (Fig. 1D). These findings provide insights into the molecular mechanisms underlying the tumor suppressive effect of LKB1, suggesting that ME3 is a direct binding partner of LKB1 in ovarian cancer cells.

LKB1 and ME3 additively increase apoptotic cell death

In this study, we aimed to investigate the effect of LKB1 and ME3 overexpression on ovarian carcinoma cell proliferation and apoptosis. To assess cell viability, we overexpressed LKB1, ME3, or both in OVCAR-3 cells and performed an MTT assay after 48 hours. Our results showed that overexpression of LKB1 or ME3 alone reduced cell viability to approximately 45% and 42%, respectively, compared to control cells. Co-transfection of both plasmids resulted in a further decrease in cell viability (Fig. 2A, left panel). We also investigated the effects of different ratios of LKB1 (0.5 μg) and ME3 (0-0.5 μg) on cell apoptosis, and our data showed that co-transfection at ratios greater than 1:0 and 1:1 was associated with increased rates of apoptosis (Fig. 2A, right panel).

To further investigate the mutual regulation of LKB1 and ME3, we evaluated their expression levels after transient transfection of one another. Our results demonstrated that the expression of LKB1 increased with higher amounts of ME3, and a similar trend was observed for the expression of ME3 after transient transfection of LKB1 (Fig. 2B, left panel). We confirmed that the decrease in cell viability was due to apoptosis using fluorescence-activated cell sorting, and our data showed that overexpression of LKB1 or ME3 increased the apoptotic cell population compared to control cells (Fig. 2C). Co-transfection with both plasmids was more effective than transfection of either plasmid alone, indicating that LKB1 and ME3 additively repressed cell proliferation.

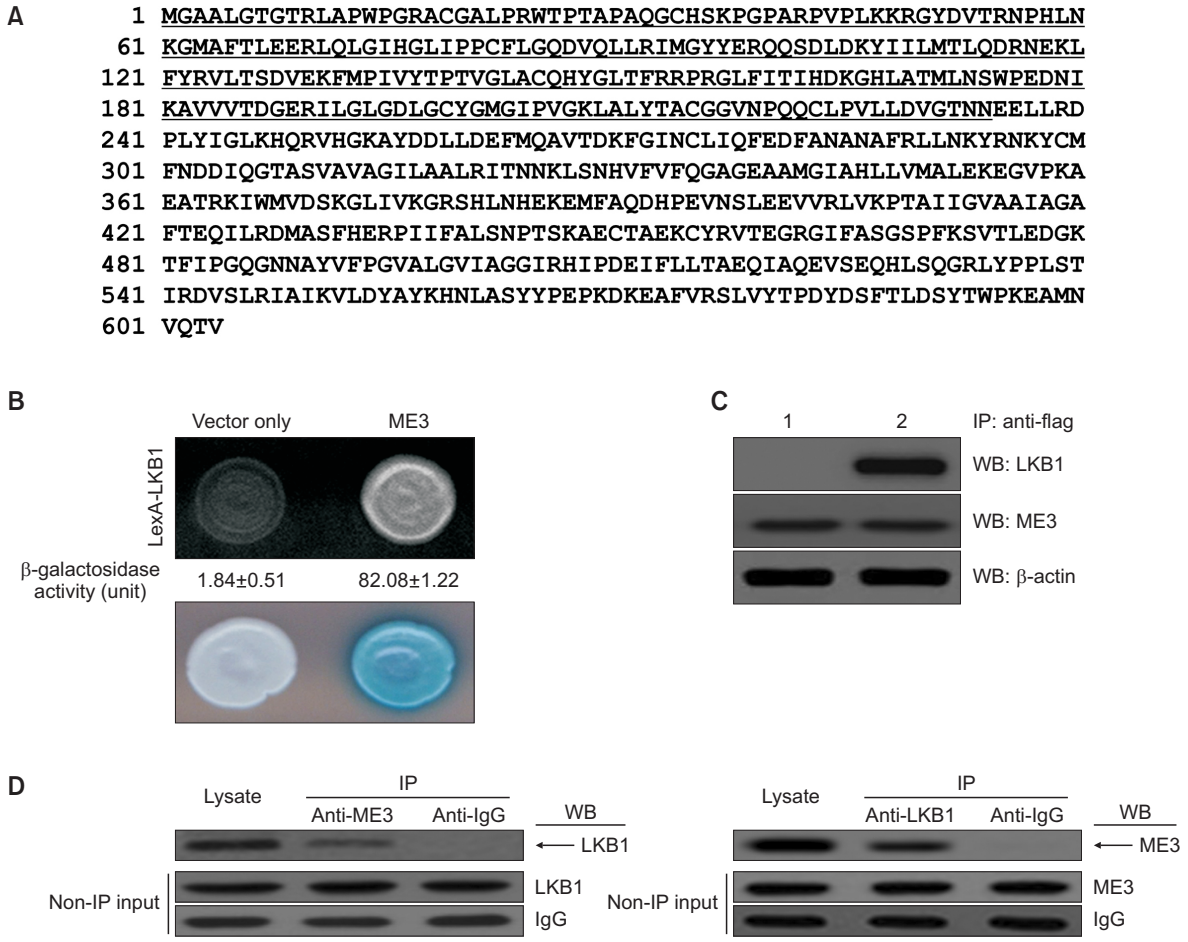

Fig. 1. Direct interaction between liver kinase B1 (LKB1) and malic enzyme 3 (ME3). (A) The amino acid sequence of ME3 is indicated using single letter abbreviations. The underlined amino acid sequence indicates the translated *Homo sapiens* ME3, isolated from the yeast two-hybrid (Y2H) assay system. (B) Positive interactions were demonstrated by observing cell growth over 3 d at 30°C on medium lacking leucine. The values of β-galactosidase activity (unit) calculated by adding o-nitrophenyl β-D-galactopyranoside are indicated below the corresponding lanes. Data are shown as the mean ± standard deviation (SD) obtained from three independent experiments. (C) Co-immunoprecipitation of LKB1 and ME3. Immunoprecipitation was performed with an anti-Flag antibody with whole cell lysates from transfected human OVCAR-3 ovarian carcinoma cells. Following immunoprecipitation, the precipitated proteins were immunoblotted with anti-LKB1 and anti-ME3 antibodies. *Lane 1*, pcDNA3.1 (vector only) and pcDNA3.1/Flag-ME3 transfected cells; lane 2, pcDNA3.1-LKB1 and pcDNA3.1/Flag-ME3 transfected cells. (D) Co-immunoprecipitation of endogenous LKB1 and ME3 in human embryonic kidney cells 293 (HEK293T) cells. All of the experiments were repeated at least three times with similar results.

Finally, we investigated the activation of caspase-3 as a potential mechanism for the mutual regulation of LKB1 and ME3. Using a caspase-3 activity assay, we found that cells transfected with LKB1, ME3, or both exhibited a significant increase in caspase-3 activation. Co-transfection with both plasmids resulted in a greater increase in caspase-3 activity compared to transfection of either plasmid alone (Fig. 2D). These findings suggest that ME3 suppresses tumor cell proliferation by augmenting LKB1-mediated apoptosis through direct interaction.

Mapping the interaction domain between human LKB1 and ME3

To identify the specific regions of LKB1 and ME3 that are involved in their interaction, three LKB1 truncation mutants and three ME3 truncation mutants were constructed and transformed into yeast cells along with full-length human ME3 or LKB1, respectively (Fig. 3A). Yeast cells containing the Leu201-Asp350 truncation mutant of LKB1 grew on selective media, indicating that this region is capable of binding to ME3. However, yeast cells transformed with the Met1-Ala200 or Glu351-Gln433 truncation mutants failed to grow, indicating that these regions are not sufficient for binding to ME3 (Fig. 3A, right panel). This result was confirmed by a β-galactosidase assay, which measures the activity of the reporter gene that is activated when LKB1 and ME3 bind (Fig. 3A).

To identify the ME3 region that binds to LKB1, three ME3 truncation mutants were constructed and transformed into yeast cells along with full-length human LKB1 (Fig. 3B, left panel, full). The β-galactosidase assay revealed that the region of ME3 that binds to LKB1 is within Met1-Tyr200 (Fig. 3B, right panel). This result was confirmed by co-transforming the Leu201-Asp350 mutant of LKB1 with one of the three ME3 mutants. Yeast cells containing the Leu201-Asp350 mutant

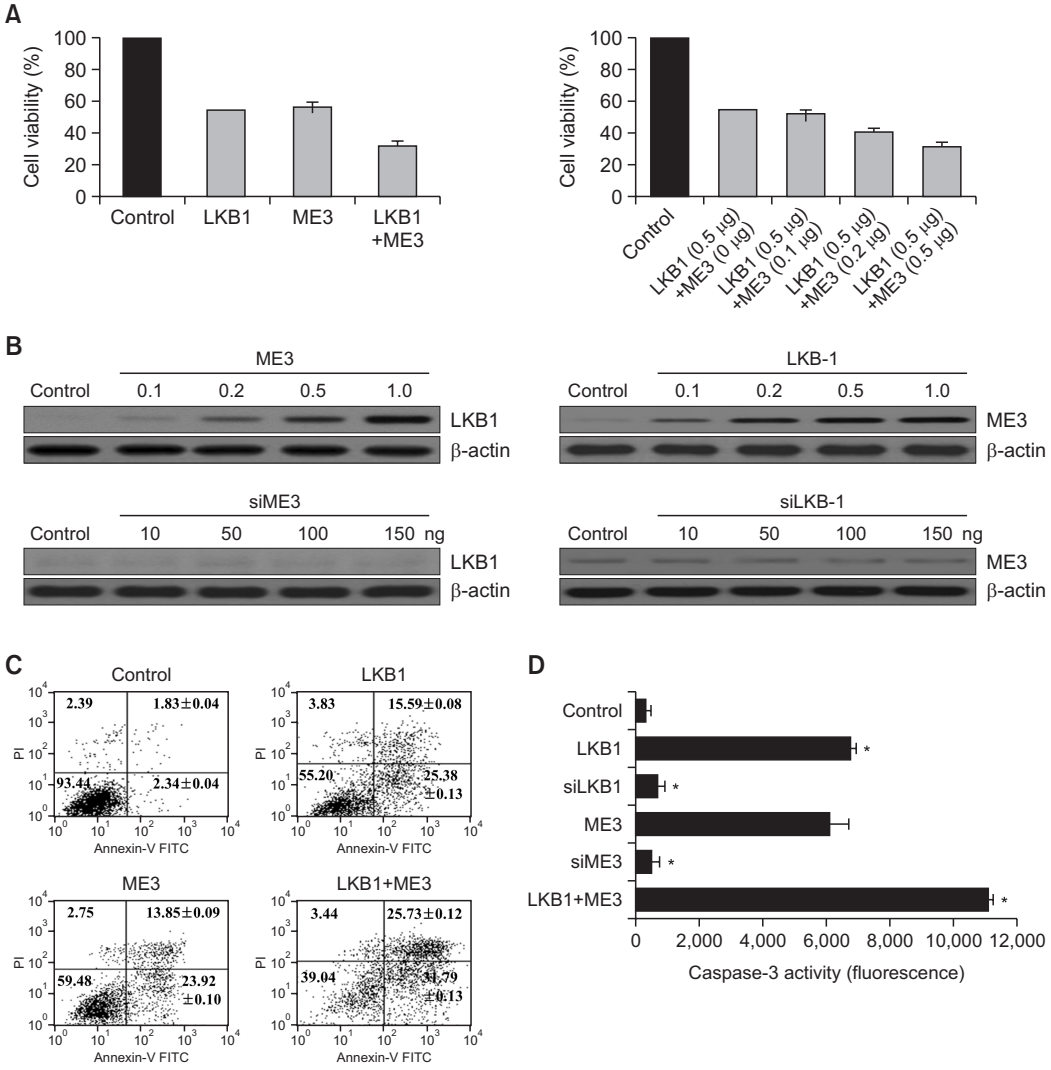

Fig. 2. LKB1 promotes the expression of ME3 and ME3-induced apoptosis in ovarian tumor cells. (A) Cell viability assay, (B) protein expression, (C) fluorescence-activated cell sorting (FACS), and (D) caspase-3 activity assay were performed with OVCAR-3 ovarian tumor cells transfected with each of the indicated cDNA constructs. Control indicates transfection with the expression vector only (empty plasmid). (A) Relative rates of cell proliferation were calculated with the 3-(4,5-dimethylthiazol-2-yl)-2.5-diphenyl-2H-tetrazolium bromide (MTT) assay. The amount of MTT formazan was determined by measuring the absorbance at 550 nm, and the sample absorbance was converted into relative proliferation rates. Data are representative of three independent experiments. (B) Cells were transfected with different concentrations of ME3 or LKB1 and whole cell lysates were prepared. Protein expression levels of LKB1 or ME3 were estimated to be the relative ratio of LKB1 or ME3 to the control by scanning densitometry. Three independent experiments revealed similar results. (C) Early and late-stage apoptotic cell death enhanced by LKB1, ME3, or LKB1 and ME3 were analyzed with fluorescein isothiocyanate (FITC)-labeled annexin V. All of the data shown are representative of three independent experiments. (D) Following transfection with LKB1, small interfering RNA (siRNA) against LKB1, ME3, siME3, or LKB1 and ME3, caspase-3 activity was measured using actyl-DEVD-7-amino-4-trifluoromethyl coumarin as the substrate. Three independent experiments were conducted in triplicate, and the bars indicate the mean ± SD; **p*<0.05 compared to the control groups.

of LKB1 with the Met1-Tyr200 ME3 mutant grew on selective media (Fig. 3C) and showed positive β-galactosidase activity, indicating that these two regions can bind to each other. However, yeast cells transformed with the Met1-Ala200 or Glu351-Gln433 ME3 mutants failed to grow (Fig. 3C) and showed no β-galactosidase activity, confirming that these regions are not sufficient for binding to LKB1.

These experiments provide evidence for the specific regions of LKB1 and ME3 that are involved in their interaction.

LKB1 and ME3 control the expression of apoptotic and cell cycle-associated regulatory proteins

In order to better understand the biological effects of LKB1 and ME3 in inducing apoptosis, we conducted an experiment to investigate the expression of proteins involved in cell cycle progression in OVCAR-3 cells. We estimated the transcriptional activity of these proteins using a luciferase activity assay. After transfecting OVCAR-3 cells with LKB1 or ME3, we measured the expression of cyclin D1 and cyclin-dependent kinase 4 (CDK4). The expression levels of cyclin D1 and

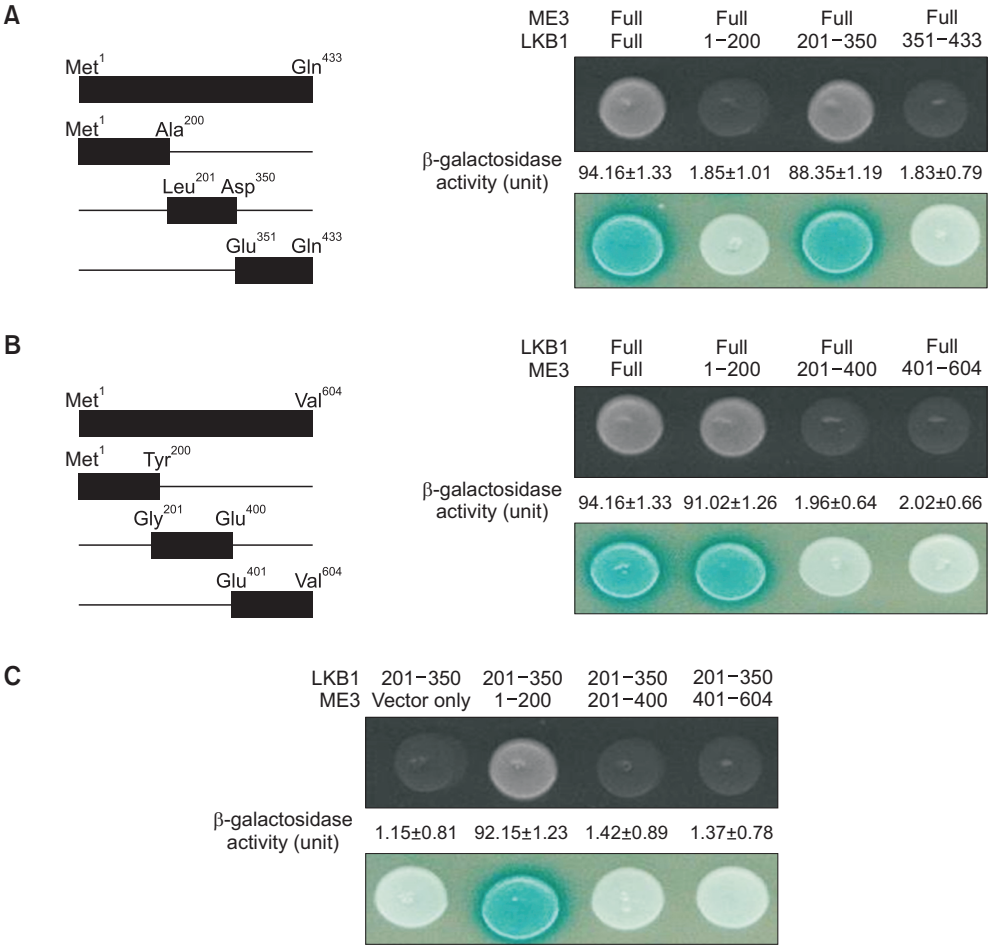

Fig. 3. Deletion mapping of the interaction domain between LKB1 and ME3 with the Y2H assay in vivo. (A) Left panel shows a schematic representation of the cDNA constructs for the full-length *LKB1* and each *LKB1* truncation. Right panel demonstrates the formation of a blue colony on a plate containing X-gal using Y2H analysis. (B) Left panel shows a schematic representation of the cDNA constructs for the full-length *ME3* and each *ME3* truncation. Right panel shows the result of a protein-protein interaction identified with the Y2H system. (C) Interaction between the LKB1 Leu^{201}–Asp^{350} truncation and three ME3 truncations, Met^{1}–Tyr^{200}, Gly^{201}–Glu^{400}, and Glu^{401}–Val^{604}, in the Y2H assay. Three independent experiments demonstrated similar results.

CDK4 were decreased upon LKB1 or ME3 transfection in the cells. However, upon transfection of LKB1 or ME3 small interfering RNA (siRNA) into the cells, the expression levels of cyclin D1 and CDK4 were restored, as shown in Fig. 4A and 4B (Fig. 4A, 4B). Additionally, the expression of p53 and p21, both involved in cell cycle regulation and apoptosis, was increased in cells transfected with LKB1 or ME3, while the expression of Bcl-2 and NF-κB, two anti-apoptotic proteins, was reduced (Fig. 4A, 4B).

These findings were confirmed through a luciferase reporter gene activity assay, which demonstrated that LKB1 and/or ME3 overexpression significantly increased the transcription of p53 and p21, while decreasing the transcription of Bcl-2 and NF-κB (Fig. 4C, 4D).

These results suggest that LKB1 and ME3 overexpression may induce apoptosis in OVCAR-3 cells by regulating the transcription of key proteins involved in cell cycle progression and apoptosis.

Phosphorylation of Akt/mTOR signaling factors is inhibited by LKB1 and ME3

The experiment aimed to investigate the impact of LKB1 and ME3 on the PI3K/mTOR/4E-BP1 signaling pathways in OVCAR-3 tumor cells, which regulate cell proliferation, protein synthesis, and angiogenesis (Guertin and Sabatini, 2005; Ma and Blenis, 2009; Jeon, 2016; Saxton and Sabatini, 2017; Sun and Song, 2021).

We transfected OVCAR-3 cells with LKB1, ME3, or both, and observed a significant decrease in the phosphorylation of PI3K, which was similar to the effect of PI3K inhibitors wortmannin and LY294002 (Fig. 5A). The inhibition of PI3K activity led to a reduction in the phosphorylation and overall levels of Akt, a downstream target of PI3K (Fig. 5B). Additionally, we investigated the involvement of upstream and downstream components of Akt/mTOR, including PDK1, TSC-2, p70S6K, GSK-3β, and 4E-BP1. The results showed that the phosphorylation of mTOR/4E-BP1 was suppressed by the expression of LKB1 and ME3 (Fig. 5B).

These results suggest that LKB1 and ME3 repressed tu-

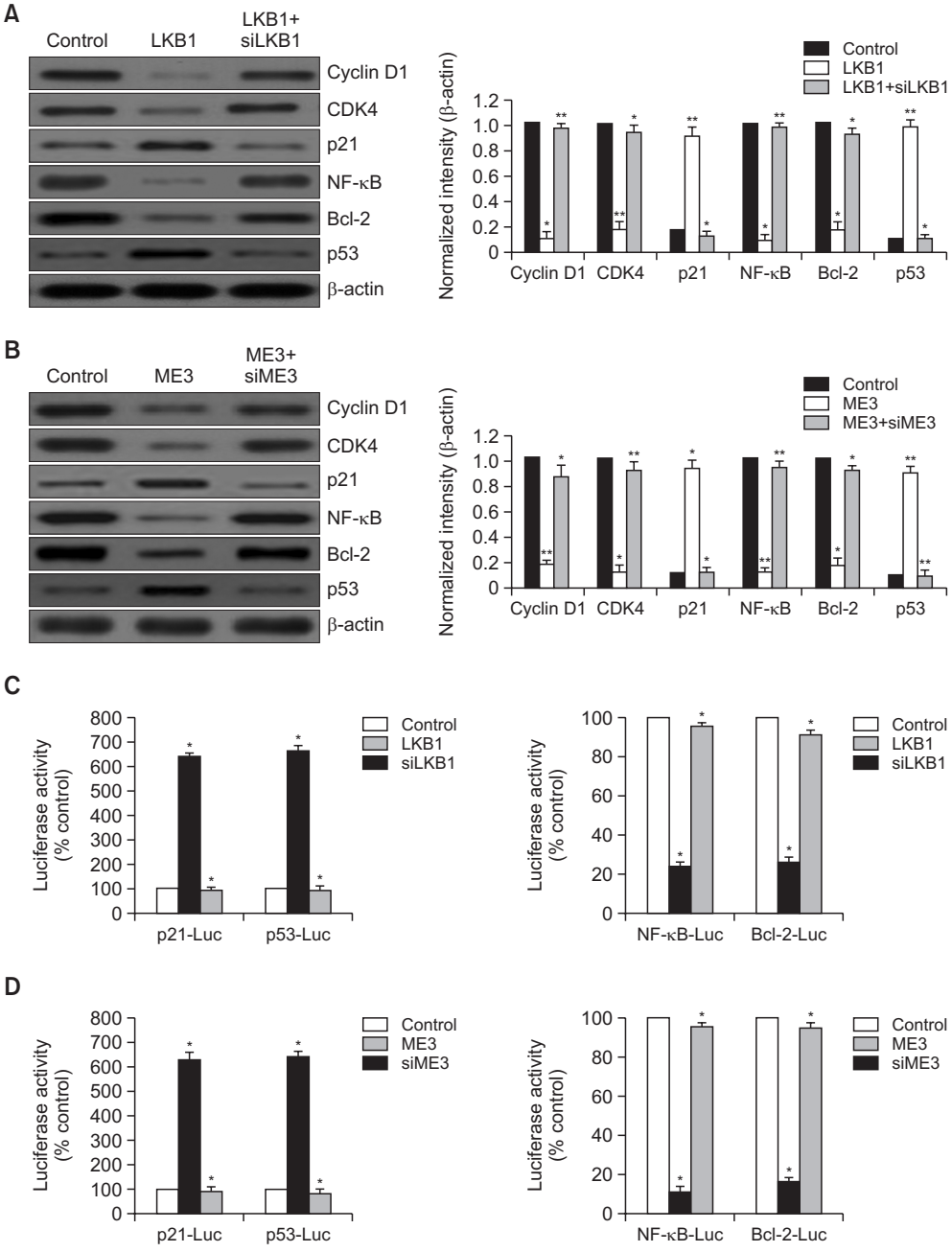

Fig. 4. LKB1 and ME3 control the expression of apoptotic- and cell cycle-associated regulatory proteins. (A, B) Cells were transfected with control, LKB1, and LKB1 and siLKB1, or control, ME3, and ME3 and siME3. Whole cell lysates were immunoblotted with primary antibodies against cell cycle-related proteins and apoptotic proteins as well as nuclear factor kappa-light-chain-enhancer of activated B cells (NF-κB). Protein expression was calculated with densitometry and normalized to the loading control. Data are expressed as the mean ± SD. **p*<0.05 and ***p*<0.01 compared to the control groups. (C, D) Promoter-luciferase activities of p21, p53, NF-κB, and B-cell lymphoma 2 (Bcl-2) were estimated using a reporter-gene assay with the p21 promoter reporter (p21-Luc), p53 promoter reporter (p53-Luc), NF-κB promoter reporter (NF-κB-Luc), and Bcl-2 promoter reporter (Bcl-2-Luc), respectively. To correct for the differences in transient transfection efficiencies, the luciferase activity was normalized by co-transfection with the *Renilla* luciferase expression plasmid. All of the data are representative of three independent experiments. Data are shown as the mean ± SD. **p*<0.05 compared to the control groups.

mor cell growth via PI3K/mTOR/4E-BP1-dependent signaling pathways in ovarian tumorigenesis.

DISCUSSION

This study investigated the role and mechanisms of LKB1 and ME3 in regulating apoptosis and cell cycle progression in ovarian tumorigenesis. The findings suggest that LKB1 and

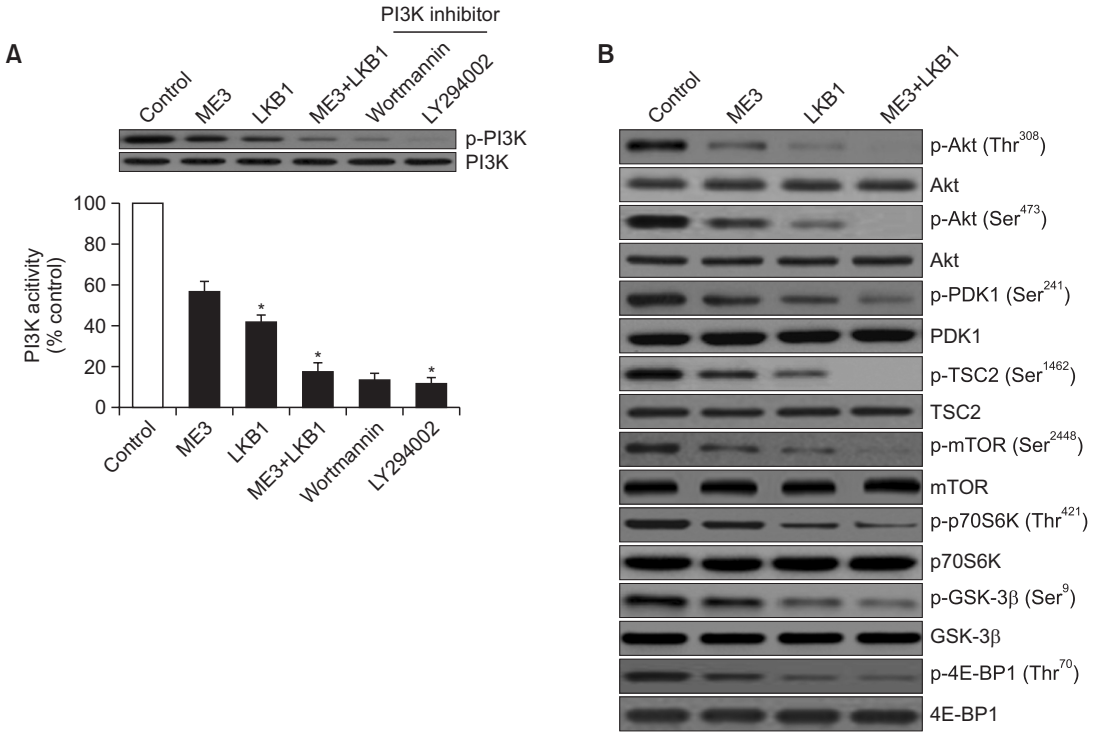

Fig. 5. Phosphorylation of Akt/mTOR signaling factors is inhibited by LKB1 and ME3. (A) The effects of LKB1 and ME3 on phosphatidylinositol 3-kinase (PI3K) activity were assessed with an *in vitro* PI3K assay (lower panel). Cells were transfected with the control (empty plasmid), ME3, LKB1, or ME3 and LKB1, and wortmannin or LY294002, two well-known PI3K inhibitors were added. After 24 h, whole cell lysates were subjected to immunoblotting to assess PI3K phosphorylation. PI3K was used as a loading control (upper panel). The experiment was performed three times. Significant differences in 95% confidence ($p<0.05$) are depicted with an asterisk (*). (B) Following transfection with the indicated expression plasmids, protein extracts (25 mg) were prepared and separated by sodium dodecyl sulfate polyacrylamide gel electrophoresis (SDS-PAGE). The proteins that were electroblotted on nitrocellulose membranes were probed with antibodies against phospho-Akt (Thr308), phospho-Akt (Ser473), phospho-PDK1 (Ser241), phospho-TSC2 (Ser1462), phospho-mTOR (Ser2448), p70S6K (Thr421), phospho-GSK-3β (Ser9), and phospho-4E-BP1 (Thr70). Non-phosphorylated protein was used as a loading control (Akt, PDK1, TSC2, mTOR, p70S6K, GSK-3β, or 4E-BP1). All of the experiments were performed at least three times with similar results.

ME3 play critical roles in these processes and dysregulation of these proteins may contribute to tumorigenesis.

The study identified a direct interaction between LKB1 and ME3 and found that LKB1 and ME3 target the PI3K/mTOR/4E-BP1 signaling pathway to trigger apoptosis in ovarian tumorigenesis, highlighting the potential therapeutic value of targeting this pathway in the treatment of ovarian cancer.

The study also provides insight into the role of LKB1 in gynecological cancers. Loss of LKB1 expression has been identified as an early event in high-grade serous ovarian tumor development, and LKB1 mutations have been found in cervical tumors, suggesting that dysregulation of LKB1 may be a contributing factor in the development of various types of gynecological cancers (Wingo *et al*., 2009; Avilés-Salas *et al*., 2023).

Our study is consistent with recent research indicating that miRNAs may play a role in the development of ovarian tumors. In particular, mature miR-17 appears to target the LKB1-p53-p21/WAF1 pathway, which can result in epigenetic alterations that promote tumorigenesis (Liu *et al*., 2015).

LKB1 interacts with PTEN to inhibit cell proliferation and survival and represses anti-apoptotic factors to inhibit cell survival (Mehenni *et al*., 2005). In addition, LKB1 represses anti-apoptotic factors, including STAT3, JNK, c-myc, k-ras, MAPK, and cyclooxygenase-2, to inhibit cell survival (Rossi *et al*., 2002; Alessi *et al*., 2006; Partanen *et al*., 2007; Zhao and Xu, 2014). Previous studies have suggested that the tumor suppressor function of LKB1 results from the repression of cell cycle progression by its downstream targets, such as Brg1, p21, p27, and cyclin D1 (Marignani *et al*., 2001; Tiainen *et al*., 2002; Liang *et al*., 2007; Scott *et al*., 2007). In our study, LKB1 and ME3 overexpression increased the expression of p53 and p21 while repressing Bcl-2 and NF-κB expression in ovarian tumor cells (Fig. 4B, 4D). LKB1 and ME3 also additively suppressed cell proliferation, with ME3-transfected cells exhibiting around 42% suppression compared to control cells.

The identification of LKB1 as a tumor suppressor gene adds to the growing body of literature on the genetic aberrations underlying ovarian tumor development (Tanwar *et al*., 2014; Wang *et al*., 2018). Loss of LKB1 expression has been identified as an early event in high-grade serous ovarian tumor development, and the current study provides further insight into the mechanisms by which LKB1 exerts its tumor suppressor function.

Furthermore, our study demonstrated that LKB1 and ME3 are involved in suppressing PI3K/Akt signaling pathway components (Fig. 5), which are crucial regulators of malignant tumors (Ishigami *et al*., 1998; Tahmatzopoulos *et al*., 2004; Ji-

ang and Liu, 2008). Our findings suggest that LKB1 and ME3 are important regulators of tumor cell proliferation, controlling key biological processes such as apoptosis, cell growth, and tumorigenesis. We also identified ME3 as a novel binding partner of LKB1, and our results suggest that LKB1 and ME3 cooperate to regulate apoptosis and contribute to the tumor suppressive function of LKB1.

In summary, our study provides important new insights into the role of LKB1 and ME3 in tumor suppression and their potential as therapeutic targets in ovarian tumorigenesis. Future studies can focus on further elucidating the molecular mechanisms underlying LKB1-mediated signaling pathways through its interaction with ME3.

CONFLICT OF INTEREST

The authors have declared that no competing interest exists.

ACKNOWLEDGMENTS

This work was supported by a grant from the National Cancer Center, Korea (NCC-2112500-1 and 2210450-1) and the Basic Science Research Program and the BK21 FOUR program through the NRF (NRF-2018R1A5A2023127, and NRF-2020R1A2C3004973).

REFERENCES

Alessi, D. R., Sakamoto, K. and Bayascas, J. R. (2006) LKB1-dependent signaling pathways. *Annu. Rev. Biochem.* **75**, 137-163.

Avilés-Salas, A., Díaz-García, D. A., Lara-Mejía, L., Cardona, A. F., Orozco-Morales, M., Catalán, R., Hernández-Pedro, N. Y., Rios-Garcia, E., Ramos-Ramírez, M. and Arrieta, O. (2023) LKB1 loss assessed by immunohistochemistry as a prognostic marker to first-line therapy in advanced non-small-cell lung cancer. *Curr. Oncol.* **30**, 333-343.

Bhatt, V., Lan, T., Wang, W., Kong, J., Lopes, E. C., Wang, J., Khayati, K., Raju, A., Rangel, M., Lopez, E., Hu, Z. S., Luo, X., Su, X., Malhotra, J., Hu, W., Pine, S.,R., White, E. and Guo, J. Y. (2023) Inhibition of autophagy and MEK promotes ferroptosis in Lkb1-deficient Kras-driven lung tumors. *Cell Death & Disease* **14**, 61.

Chang, G. G. and Tong, L. (2003) Structure and function of malic enzymes, a new class of oxidative decarboxylases. *Biochemistry* **42**, 12721-12733.

Cheng, C. P., Huang, L. C., Chang, Y. L., Hsieh, C. H., Huang, S. M. and Hueng, D. Y. (2016) The mechanisms of malic enzyme 2 in the tumorigenesis of human gliomas. *Oncotarget* **7**, 41460.

Costa Rosa, L. F. B. P., Curi, R., Murphy, C. and Newsholme, P. (1995) Effect of adrenaline and phorbol myristate acetate or bacterial lipopolysaccharide on stimulation of pathways of macrophage glucose, glutamine and O2 metabolism. Evidence for cyclic AMP-dependent protein kinase mediated inhibition of glucose-6-phosphate dehydrogenase and activation of NADP+-dependent 'malic' enzyme. *Biochem. J.* **310**, 709-714.

Dmitriev, L. (2001) Activity of key enzymes in microsomal and mitochondrial membranes depends on the redox reactions involving lipid radicals. *Membr. Cell Biol.* **14**, 649-662.

Gao, Y., Xiao, Q., Ma, H., Li, L., Liu, J., Feng, Y., Fang, Z., Wu, J., Han, X., Zhang, J., Sun, Y., Wu, G., Padera, R., Chen, H., Wong, K. K., Ge, G. and Ji, H. (2010) LKB1 inhibits lung cancer progression through lysyl oxidase and extracellular matrix remodeling. *Proc Natl Acad Sci USA* **107**, 18892-18897.

Guertin, D. A. and Sabatini, D. M. (2005) An expanding role for mTOR in cancer. *Trends Mol. Med.* **11**, 353-361.

Gurumurthy, S., Xie, S. Z., Alagesan, B., Kim, J., Yusuf, R. Z., Saez, B., Tzatsos, A., Ozsolak, F., Milos, P., Ferrari, F., Park, P. J., Shirihai, O. S., Scadden, D. T. and Bardeesy, N. (2010) The Lkb1 metabolic sensor maintains haematopoietic stem cell survival. *Nature* **468**, 659-663.

Hardie, D. G., Ross, F. A. and Hawley, S. A. (2012) AMPK: a nutrient and energy sensor that maintains energy homeostasis. *Nat. Rev. Mol. Cell Biol.* **13**, 251-262.

Hardie, D. G. (2013) The LKB1-AMPK pathway-friend or foe in cancer? *Cancer Cell* **23**, 131-132.

Hasan, N. M., Longacre, M. J., Stoker, S. W., Kendrick, M. A. and MacDonald, M. J. (2015) Mitochondrial malic enzyme 3 is important for insulin secretion in pancreatic β-cells. *Mol. Endocrinol.* **29**, 396-410.

Huynh, M. K. Q., Kinyua, A. W., Yang, D. J. and Kim, K. W. (2016) Hypothalamic AMPK as a regulator of energy homeostasis. *Neural Plast.* **2016**, 2754078.

Infante, J. P. and Huszagh, V. A. (1998) Analysis of the putative role of 24-carbon polyunsaturated fatty acids in the biosynthesis of docosapentaenoic (22:5n-6) and docosahexaenoic (22:6n-3) acids. *FEBS Lett.* **431**, 1-6.

Ishigami, S. I., Arii, S., Furutani, M., Niwano, M., Harada, T., Mizumoto, M., Mori, A., Onodera, H. and Imamura, M. (1998) Predictive value of vascular endothelial growth factor (VEGF) in metastasis and prognosis of human colorectal cancer. *Br J Cancer* **78**, 1379-1384.

Jeon, S. M. (2016) Regulation and function of AMPK in physiology and diseases. *Exp. Mol. Med.* **48**, e245-e245.

Jiang, B. H. and Liu, L. Z. (2008) AKT signaling in regulating angiogenesis. *Curr Cancer Drug Targets* **8**, 19-26.

Kang, G. J., Park, J. H., Kim, H. J., Kim, E. J., Kim, B., Byun, H. J., Yu, L., Nguyen, T. M., Nguyen, T. H., Kim, K. S., Huy, H. P., Rahman, M., Kim, Y. H., Jang, J. Y., Park, M. K., Lee, H., Choi, C. I., Lee, K., Han, H. K., Cho, J., Rho, S. B. and Lee, C. H. (2022) PRR16/Largen induces epithelial-mesenchymal transition through the interaction with ABI2 leading to the activation of ABL1 kinase. *Biomol. Ther. (Seoul)* **30**, 340-347.

Katipally, R. R., Spurr, L. F., Gutiontov, S.I., Turchan, W. T., Connell, P., Juloori, A., Malik, R., Binkley. M. S., Jiang, A. L., Rouhani, S. J., Chervin, C. S., Wanjari, P., Segal, J. P., Ng, V., Loo, B. W., Gomez, D. R., Bestvina, C. M., Vokes, E. E., Ferguson, M. K., Donington, J. S., Diehn, M. and Pitroda, S. P. (2023) STK11 Inactivation Predicts Rapid Recurrence in Inoperable Early-Stage Non–Small-Cell Lung Cancer. *JCO Precision Oncol.* **7**, e2200273.

Konen, J., Wilkinson, S., Lee, B., Fu, H., Zhou, W., Jiang, Y. and Marcus, A. I. (2016) LKB1 kinase-dependent and-independent defects disrupt polarity and adhesion signaling to drive collagen remodeling during invasion. *Mol. Biol. Cell* **27**, 1069-1084.

Liang, J., Shao, S. H., Xu, Z.-X., Hennessy, B., Ding, Z., Larrea, M., Kondo, S., Dumont, D. J., Gutterman, J. U., Walker, C. L., Slingerland, J. M. and Mills, G. B. (2007) The energy sensing LKB1–AMPK pathway regulates p27kip1 phosphorylation mediating the decision to enter autophagy or apoptosis. *Nat. Cell Biol.* **9**, 218-224.

Liu, T., Qin, W., Hou, L. and Huang, Y. (2015) MicroRNA-17 promotes normal ovarian cancer cells to cancer stem cells development via suppression of the LKB1-p53-p21/WAF1 pathway. *Tumor Biol.* **36**, 1881-1893.

Marignani, P. A., Kanai, F. and Carpenter, C. L. (2001) LKB1 associates with Brg1 and is necessary for Brg1-induced growth arrest. *J. Biol. Chem.* **276**, 32415-32418.

Ma, X. M. and Blenis, J. (2009) Molecular mechanisms of mTOR-mediated translational control. *Nat. Rev. Mol. Cell Biol.* **10**, 307-318.

Mehenni, H., Lin-Marq, N., Buchet-Poyau, K., Reymond, A., Collart, M. A., Picard, D. and Antonarakis, S. E. (2005) LKB1 interacts with and phosphorylates PTEN: a functional link between two proteins involved in cancer predisposing syndromes. *Hum. Mol. Genet.* **14**, 2209-2219.

Men, Y., Zhang, A., Li, H., Jin, Y., Sun, X., Li, H. and Gao, J. (2015) LKB1 regulates cerebellar development by controlling sonic hedgehog-mediated granule cell precursor proliferation and granule cell migration. *Sci. Rep.* **5**, 16232.

Mihaylova, M. M. and Shaw, R. J. (2011) The AMPK signalling path-

way coordinates cell growth, autophagy and metabolism. *Nat. Cell Biol.* **13**, 1016-1023.

Oakhill, J. S., Scott, J. W. and Kemp, B. E. (2012) AMPK functions as an adenylate charge-regulated protein kinase. *Trends Endocrinol. Metab.* **23**, 125-132.

Omori, Y., Ono, Y., Morikawa, T., Motoi, F., Higuchi, R., Yamamoto, M., Hayakawa, Y., Karasaki, H., Mizukami, Y., Unno, M. and Furukawa, T. (2023) Serine/Threonine Kinase 11 plays a canonical role in malignant progression of KRAS-mutant and GNAS-wild-type intraductal papillary mucinous neoplasms of the pancreas. *Ann. Surg.* **277**, e384-e395.

Partanen, J. I., Nieminen, A. I., Mäkelä, T. P. and Klefstrom, J. (2007) Suppression of oncogenic properties of c-Myc by LKB1-controlled epithelial organization. *Proc. Natl. Acad. Sci. U. S. A.* **104**, 14694-14699.

Ren, J.-G., Seth, P., Clish, C. B., Lorkiewicz, P. K., Higashi, R. M., Lane, A. N., Fan, T. W.-M. and Sukhatme, V. P. (2014) Knockdown of malic enzyme 2 suppresses lung tumor growth, induces differentiation and impacts PI3K/AKT signaling. *Sci. Rep.* **4**, 5414.

Ren, J.-G., Seth, P., Everett, P., Clish, C. B. and Sukhatme, V. P. (2010) Induction of erythroid differentiation in human erythroleukemia cells by depletion of malic enzyme 2. *PLoS One* **5**, e12520.

Rho, S. B., Lee, S. H., Byun, H. J., Kim, B. R. and Lee, C. H. (2020) IRF-1 inhibits angiogenic activity of HPV16 E6 oncoprotein in cervical cancer. *Int. J. Mol. Sci.* **21**, 7622.

Rho, S. B., Byun, H. J., Kim, B. R. and Lee, C. H. (2021) Knockdown of LKB1 sensitizes endometrial cancer cells via AMPK activation. *Biomol. Ther.* **29**, 650.

Rho, S. B., Byun, H.-J., Kim, B.-R. and Lee, C. H. (2022) Snail promotes cancer cell proliferation via its interaction with the BIRC3. *Biomol. Ther. (Seoul)* **30**, 380-388.

Rho, S. B., Kim, B.-R. and Kang, S. (2011) A gene signature-based approach identifies thioridazine as an inhibitor of phosphatidylinositol-3′-kinase (PI3K)/AKT pathway in ovarian cancer cells. *Gynecol. Oncol.* **120**, 121-127.

Rho, S. B., Lee, K. W., Lee, S.-H., Byun, H. J., Kim, B.-R. and Lee, C. H. (2021) Novel anti-angiogenic and anti-tumour activities of the N-terminal domain of NOEY2 via binding to VEGFR-2 in ovarian cancer. *Biomol. Ther. (Seoul)* **29**, 506-518.

Rossi, D. J., Ylikorkala, A., Korsisaari, N., Salovaara, R., Luukko, K., Launonen, V., Henkemeyer, M., Ristimäki, A., Aaltonen, L. A. and Mäkelä, T. P. (2002) Induction of cyclooxygenase-2 in a mouse model of Peutz–Jeghers polyposis. *Proc. Natl. Acad. Sci. U. S. A.* **99**, 12327-12332.

Saxton, R. A. and Sabatini, D. M. (2017) mTOR signaling in growth, metabolism, and disease. *Cell* **168**, 960-976.

Scott, K. D., Nath-Sain, S., Agnew, M. D. and Marignani, P. A. (2007) LKB1 catalytically deficient mutants enhance cyclin D1 expression. *Cancer Res.* **67**, 5622-5627.

Shackelford, D. B. and Shaw, R. J. (2009) The LKB1–AMPK pathway: metabolism and growth control in tumour suppression. *Nat. Rev. Cancer* **9**, 563-575.

Steinberg, G. R. and Kemp, B. E. (2009) AMPK in health and disease. *Physiological. Rev.* **89**, 1025-1078.

Sun, Y., Li, Z. and Song, K. (2021) AR-mTOR-SRF axis regulates HMMR expression in human prostate cancer cells. *Biomol. Ther. (Seoul)* **29**, 667-677.

Tahmatzopoulos, A., Rowland, R. G. and Kyprianou, N. (2004) The role of α-blockers in the management of prostate cancer. *Expert Opin Pharmacother* **5**, 1279-1285.

Tanwar, P. S., Mohapatra, G., Chiang, S., Engler, D. A., Zhang, L., Kaneko-Tarui, T., Ohguchi Y., Birrer, M. J. and Teixeira, J. M. (2014) Loss of LKB1 and PTEN tumor suppressor genes in the ovarian surface epithelium induces papillary serous ovarian cancer. *Carcinogenesis* **35**, 546-553.

Tiainen, M., Vaahtomeri, K., Ylikorkala, A. and Mäkelä, T. P. (2002) Growth arrest by the LKB1 tumor suppressor: induction of p21WAF1/CIP1. *Hum. Mol. Genet.* **11**, 1497-1504.

Wang, Y., Li, N., Jiang, W., Deng, W., Ye, R., Xu, C., Qiao, Y., Sharma, A., Zhang, M., Hung, M. C. and Lin, S. H. (2018) Mutant LKB1 confers enhanced radiosensitization in combination with trametinib in KRAS-mutant non-small cell lung cancer. *Clin. Cancer Res.* **24**, 5744-5756.

Wang, Y. P., Sharda, A., Xu, S. N., Van Gastel, N., Man, C. H., Choi, U., Leong, W. Z., Li, X. and Scadden, D. T. (2021) Malic enzyme 2 connects the Krebs cycle intermediate fumarate to mitochondrial biogenesis. *Cell Metabol.* **33**, 1027-1041.e8.

Wei, S., LiVolsi, V. A., Brose, M. S., Montone, K. T., Morrissette, J. J. and Baloch, Z. W. (2016) STK11 mutation identified in thyroid carcinoma. *Endocrine Pathol.* **27**, 65-69.

Wen, D., Liu, D., Tang, J., Dong, L., Liu, Y., Tao, Z., Wan, J., Gao, D., Wang, L., Sun, H., Fan, J. and Wu, W. (2015) Malic enzyme 1 induces epithelial–mesenchymal transition and indicates poor prognosis in hepatocellular carcinoma. *Tumor Biol.* **36**, 6211-6221.

Wingo, S. N., Gallardo, T. D., Akbay, E. A., Liang, M. C., Contreras, C. M., Boren, T., .Shimamura, T., ,Miller, D. S., , Sharpless, N. E., Bardeesy, N., Kwiatkowski, D.J., Schorge, J.O., Wong K. and Castrillon, D. H. (2009) Somatic LKB1 mutations promote cervical cancer progression. *PloS one,* **4**, e5137.

Yang, Z., Lanks, C. W. and Tong, L. (2002) Molecular mechanism for the regulation of human mitochondrial NAD (P)+-dependent malic enzyme by ATP and fumarate. *Structure* **10**, 951-960.

Zagórska, A., Deak, M., Campbell, D. G., Banerjee, S., Hirano, M., Aizawa, S., Prescott, A. R. and Alessi, D. R. (2010) New roles for the LKB1-NUAK pathway in controlling myosin phosphatase complexes and cell adhesion. *Sci. Signal.* **3**, ra25.

Zhang, W., Wang, Q., Song, P. and Zou, M.-H. (2013) Liver kinase b1 is required for white adipose tissue growth and differentiation. *Diabetes* **62**, 2347-2358.

Zhang, Y., Shi, J., Luo, J., Liu, C. and Zhu, L. (2023) Metabolic heterogeneity in early-stage lung adenocarcinoma revealed by RNA-seq and scRNA-seq. *Clin Transl Oncol.* 1-12.

Zhao, R.-X. and Xu, Z.-X. (2014) Targeting the LKB1 tumor suppressor. *Curr. Drug Targets* **15**, 32-52.